The orientation of 2,2′-bipyridine adsorbed at a SERS-active Au(1 1 1) electrode surface

A.G. Brolo [a,*], Z. Jiang [b], D.E. Irish [b]

[a] Department of Chemistry, University of Victoria, P.O. Box 3065, Victoria, BC, Canada V8W 3V6
[b] Guelph-Waterloo Centre for Graduate Work in Chemistry, Waterloo Campus, Department of Chemistry, University of Waterloo, Waterloo, ON, Canada N2L 3G1

Abstract

Surface-enhanced Raman scattering (SERS) spectra from 2,2′-bipyridine (22BPY) adsorbed on a SERS-active Au(1 1 1) electrode at several applied potentials were obtained. The SERS-active Au(1 1 1) surface was prepared following an electrochemical cleaning procedure. This procedure involves the application of continuous oxidation–reduction cycles (orcs) within a potential region where no significant surface structural changes are expected to occur. The adsorbed 22BPY may assume several conformations, including the cis- and trans-configurations. Normal Raman spectra of aqueous 22BPY at several different acidities are presented. These spectra are compared to the Raman features of both the 'free' 22BPY and its Zn complex in the solid state. The normal Raman experiments showed that unique spectral characteristics were distinguishable for both the cis- and trans-configurations. Based on these results, the potential-dependent orientation (conformation) of 22BPY adsorbed on a SERS-active Au(1 1 1) has been established. The SERS results suggested that, at a positively-charged surface, 22BPY adsorbs end-on, using both nitrogens (cis-configuration). Although no strong spectroscopic evidence suggesting potential-induced reorientation was found, the pyridine rings may no longer be coplanar at the negatively-charged surface. However, the molecules keep the upright position with both nitrogens pointing towards the surface even in these negative limits.
© 2003 Elsevier Science B.V. All rights reserved.

Keywords: Surface-enhanced Raman scattering (SERS); Au(1 1 1); Bipyridine; Molecular orientation; Raman spectroscopy; Surface spectroscopy

1. Introduction

2,2′-Bipyridine (22BPY) and its derivatives are among the most widely utilized class of ligands in coordination chemistry [1]. Metal–22BPY complexes have been investigated in the context of numerous applications, including photocatalytic systems [2], electroluminescent devices [3], solar cells [4], and DNA repair schemes [5]. 22BPY can assume several conformations, as depicted in Fig. 1. In the crystalline state, 22BPY display a S-trans-planar conformation (Fig. 1a) and thus it presents a C_{2h} symmetry [6]. When incorporated into metal complexes, 22BPY functions as a bidentate ligand [7] (chelate effect). In these cases it exists in a cis coplanar conformation (Fig. 1b) and has C_{2v} symmetry. Lower symmetry conformations must exist between these two extremes (an example is given in Fig. 1c). In solution [8,9] the molecule is in its transoidal-conformation, in agreement with quantum chemical calculations [10]. The
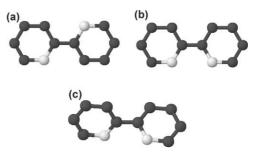

Fig. 1. Possible conformations for 22BPY. (a) trans-Configuration; (b) cis-configuration; (c) cisoid-(twisted) configuration with a torsion angle of approximately 40°.

* Corresponding author: Tel.: +1-250-721-7167; fax: +1-250-721-7147.
E-mail address: agbrolo@uvic.ca (A.G. Brolo).

slightly twisted *cis*-form is stabilized on formation of the monoprotonated 22BPY ($pK_{a1} = 4.25$ [11]) [9,12].

The number of reports on the electrochemical behaviour of 22BPY adsorbed on metallic surfaces is relatively small, considering all the attention devoted to compounds involving its interaction with metal cations. The adsorption of 22BPY at the Au(1 1 1) solution interface has been studied using cyclic voltammetry, a.c. voltammetry, chronocoulometry, and second-harmonic generation [13]. These results suggested that 22BPY is adsorbed in a flat orientation, with the two aromatic rings parallel to the gold surface, at the negatively-charged interface. It was also concluded that the molecules assume a vertical orientation at the positively-charged surface, with the two nitrogen atoms of the coplanar *cis*-conformation (as in Fig. 1b) acting in the binding between the molecule and the surface. The transition from the flat to the vertical orientation is thought to be gradual, passing through a series of intermediate states. The variation of the surface excess with the electrode potential was measured [13].

In situ scanning tunnelling microscopy (STM) has been used to study the adsorption of 22BPY on Au(1 1 1) in an electrochemical environment [14–16]. These imaging works demonstrated a 2D-phase transition in the 22BPY adlayer at the positively-charged Au(1 1 1) surface. Under these conditions, the STM images showed that the stacked 22BPY molecules assembled into rows ('rolls of coins'). The consequent supra molecular ordering, achieved due to the interaction between these rows, is a good example of electrochemically-driven organisation. This previous imaging work has sparked a series of papers on the molecular orientation (probed by Fourier transformed infrared (FTIR) techniques) and super molecular organisation (probed by STM) of 22BPY on both Au(1 1 1) [17,18] and Au(1 0 0) [19] electrode surfaces. It is a consensus among all these papers [14–19] that 22BPY adsorbs perpendicular to the positively-charged gold surface. The molecule assumes a *cis*-configuration (Fig. 1b), with both nitrogens pointing towards the gold. However, there was little spectroscopic evidence to allow a direct assignment of the molecular orientation at the negatively-charged surface, due to the low sensitivity of FTIR-based methods to sub-monolayer amounts of adsorbate. In fact, low signal-to-noise ratios were obtained from both subtractively normalized interfacial FTIR spectroscopy [18] and surface-enhanced infrared absorption spectroscopy [17] experiments, as the surface concentration decreased in the negative potential limit.

In this work, surface-enhanced Raman spectroscopy (SERS) was used to probe the adsorption of 22BPY on a Au(1 1 1) surface in a wide potential range. SERS signals of good quality were obtained at all potentials of interest, including the negatively-charged surface region. Classically, SERS-active substrates are limited basically to Au, Ag and Cu surfaces, and require a complex (rough) surface structure [20]. Nevertheless, technological advances in key aspects of Raman instrumentation is allowing the observation of normal Raman signal from smooth metal solution interfaces [21,22], and enhanced-Raman scattering from unusual SERS substrates, such as transition metals [23]. An electrochemical SERS-activation procedure that yields a reasonable signal from practically smooth Au surfaces has been developed [24]. This procedure was successfully applied to the investigation of the adsorption of pyridine and pyrazine on a single crystalline Au(2 1 0) surface [25]. This experimental approach is further validated by the good quality of the SERS spectra obtained from a Au(1 1 1) solution interface in the absence of large scale roughness presented here.

A number of studies on the vibrational spectrum of 22BPY have been published, some include normal mode analysis [26–30]. The assignments of the modes rest on strong evidence and we shall make use of them in the discussion to follow. A symmetry change from near C_{2h} to C_{2v} is expected to occur during the adsorption process. The loss of the centre of symmetry has an impact on the observable features of the Raman spectrum, and may result in infrared–Raman coincidences. SERS spectra of 22BPY adsorbed on silver colloids [31–35], various silver films and plates [36–38], and silver electrodes [39–41] have also been reported. We are not aware of any previous SERS work involving 22BPY adsorbed on gold electrodes.

2. Experimental

2.1. Solutions

All solutions were prepared from Milli-Q water. SERS experiments were performed in 0.1 M $KClO_4$ (BDH). The $KClO_4$ was purified by calcinating at 300 °C. The salt was subsequently dissolved in ultra pure water, recrystallized twice, and dried. The 22BPY from Matheson Coleman and Bell was purified by sublimation. The solutions were purged with nitrogen for at least half an hour before taking measurements, and a gentle stream of N_2 was passed over the top of the solution during the experiments.

2.2. Electrodes

The Au(1 1 1) single crystal electrode was grown, cut, and polished according to the method described elsewhere [42]. The gold was obtained from Johnson Matthey, 99.99% pure. The electrode was mounted in a glass tube and sealed with Teflon tape. The Au(1 1 1) surface was cleaned by flaming and quenching with

Milli-Q water and then transferred to the spectroelectrochemical cell [20].

The counter electrode was a platinum wire separated from the working electrode compartment by a porous glass frit. A saturated calomel electrode (SCE) was used as the reference electrode. All potentials reported in this work are against the SCE. A Luggin capillary was used to minimise the *IR* drop.

2.3. Preparation of the SERS-active Au(1 1 1) surface

A more complete discussion of this activation procedure can be found elsewhere [24]. In brief, the clean electrode was placed in the SERS cell containing 0.1 M $KClO_4$ and 1×10^{-3} M 22BPY. The electrode was submitted to continuous cleaning cycles between -0.75 and $+1.2$ V at either 20 or 50 mV s^{-1}. The cycling was performed until a cyclic voltammogram (CV) reproduced itself from one cycle to the next. Typical CVs for Au(1 1 1) in 0.1 M $KClO_4$ solution, in the presence and absence of 22BPY, are presented in Fig. 2. The CV presented in Fig. 2a is a characteristic fingerprint for a clean Au(1 1 1) surface [43]. After the SERS experiment, the Au(1 1 1) electrode was rinsed with copious amounts of Milli-Q water, flame annealed and transferred to a clean electrochemical cell containing 0.1 M $KClO_4$
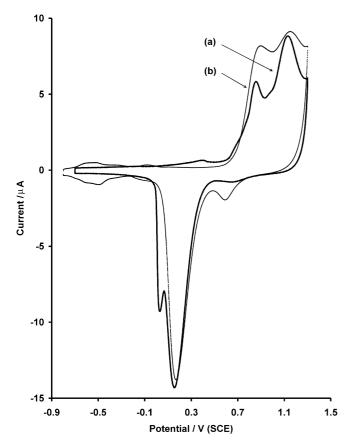

Fig. 2. CVs for a Au(1 1 1) electrode in 0.1 M $KClO_4$ solution. (a) [22BPY] = 0 M; (b) [22BPY] = 1 mM.

solution. CVs were obtained and the features presented in Fig. 2a were reproduced. This surface characterisation confirms that significant large scale roughness features have not been induced by the activation procedure. However, it is likely that atomic scale roughness and defects are the SERS-active sites for a substrate prepared according to this procedure.

2.4. Instrumentation

Raman spectra were measured with a Renishaw 1000 Raman microscope system equipped with a CCD. A macropoint accessory, with a 40-mm focal length, was used to redirect the laser light to the electrode surface in the spectroelectrochemical cell. Spectra were excited by the 632.8 nm line of a 35 mW Melles Griot He–Ne laser. The spectrometer was interfaced to a PC containing programs for data acquisition and the GRAMS/32 software. A potentiostat PAR model 273 was used in both the electrochemical and the SERS experiments.

3. Results and discussion

3.1. Normal Raman spectra

In order to infer the orientation/conformation of 22BPY adsorbed on the electrode surface, it is important to assess the Raman features that are characteristic for 22BPY in both *cis*- and *trans*-conformations. Aqueous and solid 22BPY are believed to be *trans* (Fig. 1a) [6,9]. The 22BPY conformation changes to *cis* (Fig. 1b) under either protonation or complexation with metal ions [7]. Fig. 3 shows the spectra of aqueous 22BPY solutions at different acidities. These solutions were prepared by adding drops of HCl and NaOH to a 16 mM aqueous solution of 22BPY. The pH of the original aqueous solution (16 mM 22BPY) was 7.24. Sample spectra for the range 300–1800 cm^{-1} for pH values 7.24, 2.10 and a 6 M HCl solution containing 22BPY are presented in Fig. 3a–c. The latter spectrum is that of the diprotonated 22BPY, and the spectrum on Fig. 3b corresponds to the monoprotonated species, 22BPYH^{+}. The spectral features presented in Fig. 3 agree closely with the FT-Raman data reported for 22BPY and its protonated forms [44]. The bands positions and assignments (after Refs. [26–30,34]) are presented in Table 1. The spectrum of the monoprotonated form (Fig. 3b) differs significantly from that of the aqueous 22BPY (Fig. 3a). The ring breathing mode, at 1002 cm^{-1} shifted to higher frequency (1010 and 1008 cm^{-1} in Fig. 3b and c, respectively) under protonation. The ring stretch mode at 1306 cm^{-1} split into two components at approximately 1320 and a shoulder at 1313 cm^{-1} in Fig. 3b. The relative intensities of the bands at 1449, 1489, and 1576 and 1599 cm^{-1} all
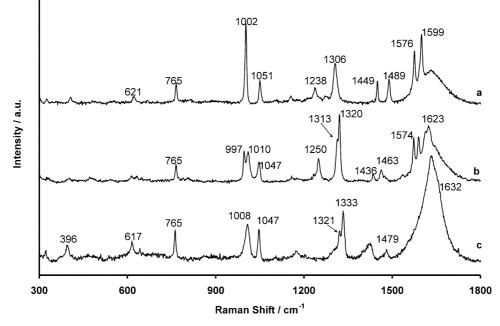
Fig. 3. Raman spectra of aqueous 22BPY solutions. (a) pH 7.24; (b) pH 2.10; (c) [HCl] = 6 M.

decreased from Fig. 3a–c. Other band positions shifted by small amounts and new bands occurred at 997, 1436 and 1623 cm^{-1} for the monoprotonated form in Fig. 3b. Strong vibrational bands corresponding to out-of-plane modes were observed neither for the *trans*- (Fig. 3a) or the *cis*-conformation (Fig. 3b). It is also important to emphasize further the changes in the relative intensities for the 22BPY in both conformations. The ring breathing mode dominated the spectrum when the molecules were *trans* (Fig. 3a). On the other hand, the ring stretch peaks at approximately 1320 cm^{-1} were stronger for the *cis*-form (Fig. 3b). The appearance of more bands in Fig. 3b is consistent with a lower symmetry for the *cisoid*-conformation [9].

Normal Raman spectra of the solid 22BPY and the solid Zn(22BPY)Cl$_2$ complex are shown in Fig. 4. Comparison between the spectra of the two solids, as shown in Fig. 4a and b, also helps in the characterisation of the two extremes of conformation. Analogous to the solution spectra presented in Fig. 3a–c, two strong peaks at 1571 and 1589 cm^{-1} due to the *trans*-form (Fig. 4a) were replaced by one strong band at 1599 cm^{-1} and a medium intensity peak at 1569 cm^{-1} in the *cis*-form (Fig. 4b). Fig. 4a also shows two strong bands at 1445 and 1481 cm^{-1}, but only one peak at 1493 cm^{-1} was observed for the *cis*-form in Fig. 4b. The absence of the peak at approximately 1445 cm^{-1} has been used as a fingerprint for the conformation of 22BPY adsorbed on silver electrodes [33]. The formation of the complex was also accompanied by several peak shifts to higher vibrational frequencies. The most affected peak was the ring breathing mode, which shifted from 994 cm^{-1}

(Fig. 4a) to 1030 cm^{-1} (Fig. 4b). The shift in the ring breathing region was not as significant in the aqueous solution spectra presented in Fig. 3a–c, indicating that the interaction between the nitrogens of the rings and the hydrogen cation is weaker than their interaction with the Zn^{2+}. Some information about the relative strength of the adsorption can be inferred by the magnitude of the upward shift of this ring breathing mode. The relative intensity changes, observed in Fig. 4a and b, were also similar to the changes observed in Fig. 3a–c. The ring breathing mode no longer dominated the spectrum of the *cis*-form in Fig. 4b, losing some of its intensity to the bands at 1314 and 1599 cm^{-1}. An out-of-plane ring deformation was observed as a weak feature at 813 cm^{-1} in Fig. 4a. This peak does not shift significantly due to the complexation. Considering the differences between the spectra of the *cis*- and *trans*-forms of 22BPY, as seen in Figs. 3 and 4 and discussed above, it is apparent that it should be possible to reach conclusions regarding the conformation of the adsorbed molecule.

3.2. SERS spectral features

SERS spectra obtained at several applied potentials (+300, 0, −300, −600, and −700 mV) are shown in Fig. 5. The intense band at 935 cm^{-1} and the bands at 462, 629, and 1113 cm^{-1} arose from the perchlorate anion, present in the electrolyte at 0.1 M. The other bands were due to the 22BPY adsorbed on the gold electrode surface. The peak positions are presented in Table 2.

Table 1
Vibrational wavenumber (cm^{-1}) for Raman spectra of solid and solution: comparison with the literature and assignments

Solid	Solution			Zn(bpy)Cl$_2$		Ru(bpy)$_2$Cl$_2$	Assignment
This work	This work (in H$_2$O)			This work	IR	Ref. [30]	
	pH 7.24	pH 2.10	[HCl] = 6 M				
		1623 s	1632 s				
		1613 s					
1589 vs	1599 vs	1590 s		1599 vs	1606 m, 1599 s	1606	ring str. (C–C, C–N)+N–H+i.p. def.
1571 vs	1576 vs	1574 s		1569 m	1576 w, 1568 w	1557	ring str. (C–C, C–N)
		1536 w					
1481s	1489 s	1475 w	1479 w	1493 vs	1492 m	1485	ring str. (C–C, C–N)+C–H i.p. def.
		1463 m			1473 s		ring str. (C–C, C–N)+C–H i.p. def.
1445 s	1449 s	1436 w	1422 w	1447 vw	1445 vs		ring str. (C–C, C–N)+C–H i.p. def.
		1320 vs	1333 s	1322 sh	1424 w		C–C inter-ring str.+ring str. (C–C, C–N)+C–H i.p. def.
1307 m	1306 vs	1313 sh	1321 sh	1314 vs	1319 m	1318	C–C inter-ring str. + ring str. (C–C, C–N)+C–H i.p. def.
1300 s				1299 vw			C–C inter-ring str. + ring str. (C–C, C–N)+C–H i.p. def.
	1276 vw	1250 s		1266 m	1266 vw, 1252 m	1272	ring str. (C–C, C–N)+C–C inter-ring str.+C–H i.p. def.
1236 s	1238 m						ring str. (C–C, C–N)+C–C inter-ring str.+C–H i.p. def.
1216 w					1222 w		ring str. (C–C, C–N)+C–C inter-ring str.+C–H i.p. def.
			1172 w	1182 vw	1178 vw, 1172 w		
1145 w	1156 w	1159 w		1158 w	1159 m	1171	C–H i.p. def.+ring str.
1092 w				1101 vw	1101 w, 1072 vw		C–H i.p. def.+ring str.
1044 m	1051 s	1047 s	1047 s	1063 m	1063 m, 1046 w		C–H i.p. def.+ring str. and def.
		1010 s	1008 s	1030 vs	1030 m, 1019 m	1027	ring breathing
994 vs	1002 vs	997 s					ring breathing
					976 w, 970 w, 904 w		
813 w	813 vw	809 vw		814 w	819 vw		C–H o.p. def.
763 m	765 s	765 m	765 s	765 m	772 vs, 733 s		i.p. ring def.
				662 vw	661 w		i.p. ring def.
				652 vw	652 w		
		631 w	642 vw	639 w	639 w		
613 m	621 w	613 w	617 w				i.p. ring def.
				547 w			
439 w		474 vw		461 w			o.p. ring def.
	407 w	404 vw	396 w		414 m		o.p. ring def.
				368 w	367 vw		i.p. ring def.
332 vw	328 w	330 vw	322 w	331 vw	331 m		ring–ring str.

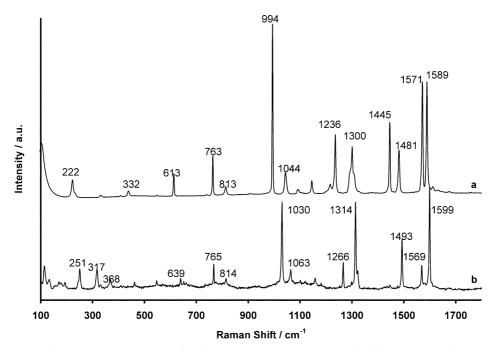str., Stretching; def., deformation; i.p., in-plane; o.p., out-of-plane.

Fig. 4. (a) Raman spectrum of solid 22BPY; (b) Raman spectrum of solid Zn(22BPY)Cl$_2$.

The totally symmetric in-plane vibrations of 22BPY were strongly enhanced upon adsorption on the SERS-active Au(1 1 1) surface (see the assignment in Table 1). The out-of-plane vibrations, e.g., 407 and 814 cm^{-1}, did not appear in the SERS spectra presented in Fig. 5 at any applied potential. The absence of bands due to the out-of-plane modes of vibrations is an indication that the molecule does not adsorb flat at the electrode surface [45]. This assumption is further corroborated by the positive shift of the ring breathing mode relative to the 'free molecule'. This mode appeared at around 1015 cm^{-1} for the adsorbed molecule (Fig. 5) compared to 1002 cm^{-1} in solution and 994 cm^{-1} in the solid (see Fig. 3a and Fig. 4a). A negative shift of the vibrational frequency of the ring breathing mode is expected for aromatic rings lying flat at the metallic surface [46]. The magnitude of the positive shift of the ring breathing mode also provides an indication of the relative strength
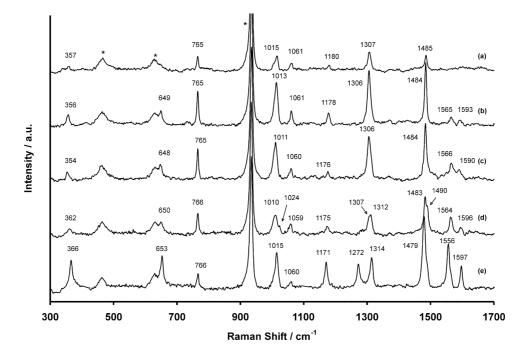

Fig. 5. SERS spectra of 22BPY adsorbed on a SERS-active Au(1 1 1) surface. (a) $E = +300$ mV; (b) $E = 0$ mV; (c) $E = -300$ mV; (d) -600 mV; (e) -700 mV. Asteriks indicates the bands due to the perchlorate ion.

Table 2
Vibrational wavenumbers (cm^{-1}) of 22BPY adsorbed on a Au(1 1 1) electrode

Electrode potential/mV (SCE)					
+300	0	−300	−600	−750	cis [a]
357 w	356 w	354 w	362 w	366 s	368 w
	649 w	648 w	650 w	653 s	652 vw
765 m	765 s	765 s	766 s	766 m	765 m
1015 m	1013 s	1011 s	1010 s	1015 s	1030 vs
			1024 sh		
1061 w	1061 m	1060 m	1059 m	1060 w	1063 w
1180 w	1178 m	1176 w	1175 w	1171 s	1182 vw
				1272 m	1266 m
1307 s	1306 s	1306 s	1307 sh		
			1312 s	1314 s	1314 vs
1485 m	1484 s	1484 s	1483 s	1479 s	1493 s
			1490 sh		
	1565 w	1566 m	1564 m	1556 s	1569 m
	1593 w	1590 w	1596 w	1597 m	1599 vs

[a] Zn(bpy)Cl$_2$.

of the surface—22BBPY interaction. The shift was approximately +13 cm^{-1} for the adsorbed molecule (Fig. 5) from the 'free molecule' in solution. This is compared to a shift of approximately +36 cm^{-1} observed for the Zn complex from solid 22BPY (Fig. 4) and approximately +8 cm^{-1} due to protonation (Fig. 3). These results suggest that the 22BPY molecule is not strongly chemisorbed. The effect of 22BPY on the conductance and mechanical properties of copper nanowires also indicates a relatively mild adsorption strength [47,48].

Table 2 includes the band positions observed for the Zn(22BPY)Cl$_2$ complex for comparison. The good correlation between the SERS spectra (Fig. 5) and the spectrum of the complex (Fig. 4b) indicates that 22BPY presents a *cisoid*-conformation on the electrode surface at all potentials studied. For instance, the bands at 613, 1236 and 1445 cm^{-1}, which are fingerprints for the *trans*-configuration, were not present in any of the spectra presented in Fig. 5. The relative intensity between the ring breathing mode at approximately 1015 cm^{-1} and the in-plane ring mode at approximately 1307 cm^{-1} was also more similar to what is observed in the spectra of 22BPY in the *cis*-configuration (Fig. 4b). However, the relative intensities from SERS spectra are expected to differ significantly from normal Raman spectra due to the specific surface selection rules [45]. Moreover, the relative intensities are also potential-dependent [20,45]. In fact, some of the SERS features measured at a negatively-charged electrode (Fig. 5c–e) are distinct from those observed in the spectra obtained at a positively-charged electrode (Fig. 5a and b). The pzc for a Au(1 1 1) surface immersed in 0.1 M KClO$_4$ solution is around +90 mV versus SCE [49]. The SERS spectrum at −700 mV (Fig. 5e) is very similar

to the resonance-Raman (RR) spectrum of Ru(22BPY)$_3^{+2}$, specially in the relative intensity distribution [30,50,51]. This is a further indication that the molecule is not in its *trans*-configuration at −700 mV. Before leaving the discussion of the negatively-charged electrode region (Fig. 5c–e), it is noted that there were two bands which increased in intensity as the potential ranged from −300 to −700 mV. These occurred at 1171 and 1479 cm^{-1}; the former shifted from the 1180 cm^{-1} band at +300 mV (Fig. 5a) and the latter seemed to develop from a low frequency shoulder on the 1485 cm^{-1} band at +300 mV. Clearly there was a multiple band structure in this region. Also at −700 mV a unique new line occurred at 1272 cm^{-1}. This band is generally present in the RR spectra of 22BPY complexes [50,51], further supporting the proposed *cis*-conformation for the adsorbed molecule.

The SER intensity for a pair of bands at 1556 and 1597 cm^{-1} diminished significantly at the positively-charged electrode. The bands were sharper (e.g. the bands at 1484 and 1306 cm^{-1}) in that potential region, suggesting only one predominant conformation. Although important changes in the relative intensities were observed, the marker bands for the *trans*-conformation were all absent. The position of the ring breathing mode and the relative intensities of the peaks indicate that 22BPY is also adsorbed in a *cis*-type conformation, oriented end-on, for potentials more positive than the pzc.

The SERS band at approximately 765 cm^{-1} did not shift significantly with the applied potential and its integrated intensities relative to the 935 cm^{-1} band of ClO$_4^-$ are plotted against the applied potential in Fig. 6. The dependence of the surface excess on the applied potential obtained electrochemically [13] is also shown in Fig. 6. Both the surface coverage and the SERS intensities increased as the potential was swept from −700 mV to more positive values. A step was observed in the region between −400 and −300 mV for the surface coverage versus potential curve (Fig. 6). This feature has been interpreted as an indication that the molecules suffer reorientation between these potentials [13]. Similar behaviour was observed in the SERS intensity versus potential curve in the range between −500 and −300 mV. This may indicate that the SERS data presented in Fig. 6 also support the hypothesis of reorientation. However, the possibility of important contributions from charge-transfer resonances to the SERS results presented in Fig. 6 cannot be completely discarded. In any case, the SERS data presented in Fig. 5 are contrary to the notion that the molecules are bonded flat (π-bonded) with a coplanar *trans*-conformation (as shown in Fig. 1a) when the potentials are in the most negative range. According to the SERS results obtained in this work, the 22BPY molecules are still in a *cisoid*-conformation at a negatively-charged electrode. The

magnitude of both the relative SERS intensity and the surface coverage (Fig. 6) increased after the shoulder under discussion as the applied potential was made more positive. The surface coverage versus potential curve reached a maximum at around 0 mV, and its value did not change as the potential became more positive (Fig. 6). The relative SERS intensity versus potential curve presented completely different behaviour in this potential region. The SERS signal reached a maximum at around 0 V, but the intensity decreased as the potential became more positive (Fig. 6). This type of behaviour has been observed for pyridine [24] and pyrazine [52], nevertheless, in these cases the SERS intensities are maximised at a surface coverage value equal to 2/3 of a monolayer. These trends observed at high surface concentration were attributed to the depolarizing fields arising from neighbouring dipoles in close proximity to a given molecule. The decrease in the relative SERS intensity presented in Fig. 6 occurred in the same potential region where a 2D-phase transition was observed by STM [17]. The supra molecular organisation of the molecules at these potentials certainly leads to a better alignment between their dipoles, which would explain the decrease in the SERS intensities even considering that the amount of molecules on the surface remains constant.

3.3. On the orientation of 22BPY adsorbed on a SERS-active Au(1 1 1) surface

Surface coverage data, obtained using electrochemical methods, showed that the surface is fully packed at potentials more positives than −200 mV (Fig. 6), indicating that the molecules are vertically oriented [13]. These results were corroborated using scanning probe microscopy techniques [14,16]. In situ infrared studies also showed that the molecule adsorb end-on, with both nitrogens facing the electrode surface [17,18]. All these data are consistent with the SERS features presented in Fig. 5 for an applied potential of +300 mV. It can be concluded that at the positively-charged electrode the 22BPY molecules are vertically oriented, in the *cis*-conformation and with both rings coplanar (as shown in Fig. 1b). The only indication obtained here that a structural change might have occurred at the negatively-charged electrode, as suggested by the electrochemical data [13], was the potential profile presented in Fig. 6. Attempts to obtain direct information on the orientation of 22BPY adsorbed on a negatively-charged Au(1 1 1) surface using in situ IR were not successful, because of the lack of sensitivity of the IR technique to detect this molecule in sub-monolayer amounts [17,18]. The SERS spectra at the negatively-charged electrode, presented in Fig. 5, were clear and indicated that the molecules were not adsorbed flat. The SERS features also undoubtedly showed that the molecule is in a

cisoid-conformation. Recent ab intio calculations involving 22BPY have demonstrated that very small changes are predicted between the vibrational spectrum of a coplanar *cis*-conformation and intermediate twisted configurations, with torsion angles between 0 and 40° [18]. The SERS result presented in Fig. 6 may suggest a transition in the molecular orientation as the electrode potential is made negative, however, SERS features due to the *trans*-conformer were not observed. It is then possible to propose that 22BPY is adsorbed in a *cis*-configuration, but with no coplanar rings, at the negatively-charged SERS-active Au(1 1 1) electrode (as shown in Fig. 1c). A non-coplanar (twisted) configuration has been suggested for 22BPY adsorbed on a Pt(1 1 1) electrode surface [53].

The formation of the twisted configuration at the negatively-charged electrode should still be more favourable energetically than the *trans*-form. The torsional energy curve for 22BPY has been calculated at both ab initio and semi-empirical levels. [10]. The calculations predicted that work of approximately 30 kJ mol^{-1} should be necessary to change the gas phase conformation from *trans* to *cis*. The energetics would be considerable different in solution (more precisely, in the metal solution interface), but it is obvious that a
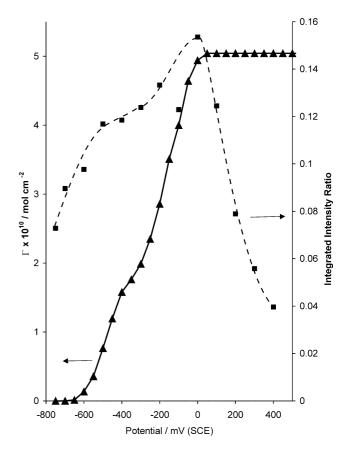

Fig. 6. (a) Surface coverage versus potential plot for 22BPY adsorbed on a Au(1 1 1) electrode—from Ref. [13]; (b) Relative SERS intensity (765 cm^{-1}-band) versus applied potential plot.

significant energy gain occurs when the molecule adsorbs end-on at the positively-charged electrode (despite the work spent on the *trans*- to *cis*-change). As the surface charge is made more negative, there are, in a first approximation, at least two factors that must be considered. One is the repulsive interaction between the lone pairs of electrons on the nitrogens and the negatively-charged surface. This effect would favour a *cis*- to *trans*-conformational change. The other factor is the tendency of both nitrogens to bind to a single Au site (chelate effect). In terms of conformational change, this effect would be contrary to the repulsive interaction. Other effects, such as the changes in the surface polarizability and the coverage-dependent intermolecular interactions may also play a role. An energy gain occurs if the molecule returns to its natural *trans*-conformation. However, the calculations also showed that intermediate twisted conformations can also be stabilized [10]. For instance, a local minimum at approximately 40° in the torsional energy curve was predicted [10]. Therefore, a twisted *cis*-conformation (as presented in Fig. 1c) for 22BPY adsorbed on Au electrode at the negatively-charged electrode can be energetically justified. It is our expectation that this work will stimulate others to pursue a more complete quantum-chemical calculation involving the interaction of 22BPY with a model Au surface (cluster or jellium).

4. Conclusions

Electrochemical SERS was used to investigate the adsorption of 22BPY on a SERS-active Au(1 1 1) electrode surface. It was demonstrated that 22BPY adsorbs end-on at the positively-charged electrode with both nitrogen groups pointing down to the surface (*cis*-configuration). This conclusion is in agreement with electrochemical, spectroscopic and imaging data reported in the literature. On the other hand, the SERS results presented here are the first direct spectroscopic evidence for the orientation of 22BPY at the negatively-charged Au electrode. The data indicates that the molecule remains adsorbed end-on in a *cisoidal*-configuration at negative potential limits. Although the SERS data did not provide strong evidence for a potential-induced reorientation, the dependence of the SERS intensity with the applied potential may suggest a change in the molecular configuration between −300 and −500 mV. It was then suggested that the molecule assumed an intermediate torsional configuration (the aromatic rings were no longer coplanar) at potentials more negative than −500 mV. Molecular quantum-chemical calculations have shown multiple minima in the torsional energy curve of 22BPY, supporting this argument. The findings reported here contrast with a previous suggestion that 22BPY adsorbs flat and in a

trans-configuration at the negatively-charged gold surface. Nevertheless, although no large scale roughness features were introduced, the Au(1 1 1) electrode was activated to became an appropriate SERS substrate. Therefore, the possibility that the results presented here represent a fraction of the 22BPY molecules adsorbed on special atomic roughness cannot be completely ignored.

References

[1] L.A. Summers, in: A.R. Katritzky (Ed.), Advances in Heterocyclic Chemistry, vol. 35, Academic Press, Orlando, 1984, p. 281.
[2] R.F. Khairutdinov, J.K. Hurst, Nature 402 (1999) 509.
[3] S. Welter, K. Brunner, J.W. Hofstraat, L. De Cola, Nature 421 (2003) 54.
[4] J. Schnadt, P.A. Bruhwller, L. Patthey, J.N. O'Shea, S. Sodergren, M. Odellus, R. Ahuja, O. Karis, M. Bassler, P. Persson, H. Slegbahn, S. Lunell, N. Matensson, Nature 418 (2002) 620.
[5] P.J. Dandliker, R.E. Holmlin, J.K. Barton, Science 275 (1997) 1465.
[6] L.L. Merrit, E.D. Schroeder, Acta Crystallogr. 9 (1956) 1981.
[7] M.A. Khan, D.G. Tuck, Acta Crystallogr. C40 (1984) 60.
[8] J.W. Emsley, J.G. Garnett, M.A. Long, L. Lunazzi, G. Spunta, C.A. Veracini, A. Zanadei, J. Chem. Soc. Perkin II (1979) 385.
[9] K. Nakamoto, J. Phys. Chem. 64 (1960) 1420.
[10] C. Jaime, J. Font, J. Mol. Struct. 195 (1989) 103.
[11] R.H. Linnell, A. Kaczmarczyk, J. Phys. Chem. 65 (1961) 1196.
[12] I.R. Beattie, M. Webster, J. Phys. Chem. 66 (1962) 115.
[13] D. Yang, D. Bizzotto, J. Lipkowski, B. Pettinger, S. Mirwald, J. Phys. Chem. 98 (1994) 7083.
[14] F. Cunha, N.J. Tao, Phys. Rev. Lett. 75 (1995) 2376.
[15] F. Cunha, N.J. Tao, X.W. Wang, Q. Jin, B. Duong, J. D'Agnese, Langmuir 12 (1996) 6410.
[16] T.h. Dretschkow, D. Lampner, T.h. Wandlowski, J. Electroanal. Chem. 458 (1998) 121.
[17] H. Noda, T. Minoha, L.-J. Wan, M. Osawa, J. Electroanal. Chem. 481 (2000) 62.
[18] M. Hoon-Khosla, W.R. Fawcett, J.D. Goddard, W.-Q. Tian, J. Lipkowski, Langmuir 16 (2000) 2356.
[19] T.h. Dretschkow, T.h. Wandlowski, J. Electroanal. Chem. 467 (2000) 207.
[20] A.G. Brolo, D.E. Irish, B.D. Smith, J. Mol. Struct. 405 (1997) 29.
[21] A.G. Brolo, M. Odziemkowski, J. Porter, D.E. Irish, J. Raman Spectrosc. 33 (2002) 136.
[22] A.G. Brolo, M. Odziemkowski, D.E. Irish, J. Raman Spectrosc. 29 (1998) 713.
[23] Z.Q. Tian, B. Ren, D.Y. Wu, J. Phys. Chem. B 106 (2002) 9463.
[24] L. Stolberg, J. Lipkowski, D.E. Irish, J. Electroanal. Chem. 300 (1991) 563.
[25] A.G. Brolo, D.E. Irish, J. Lipkowski, J. Phys. Chem. B 101 (1997) 3906.

[26] N. Neto, M. Muniz-Miranda, L. Angeloni, E. Castellucci, Spectrochim. Acta 39A (1983) 97.

[27] M. Muniz-Miranda, E. Castellucci, N. Neto, G. Sbrana, Spectrochim. Acta 39A (1983) 107.

[28] E. Castellucci, L. Angeloni, N. Neto, G. Sbrana, Chem. Phys. 43 (1979) 365.

[29] J.S. Strukl, J.L. Water, Spectrochim. Acta 27A (1971) 209.

[30] A. Basu, H.D. Gafney, T.C. Strekas, Inorg. Chem. 21 (1982) 2231.

[31] M. Kim, K. Itoh, J. Phys. Chem. 91 (1987) 126.

[32] F.-Q. Yu, C.-P. Zhang, G.-Y. Zhang, J. Raman Spectrosc. 20 (1989) 435.

[33] T.C. Strekas, P.S. Diamandopoulos, J. Phys. Chem. 94 (1990) 1986.

[34] A.L. Kamyshny, V.N. Zakharov, Y.V. Fedorov, A.E. Galashin, L.A. Aslanov, J. Colloid Interface Sci. 158 (1993) 171.

[35] V. Zakharov, A. Rumiantcev, L. Aslanov, Y. Fedorov, A. Galashin, A. Kamyshny, IS&T's 48th Annual Conference Proceedings, 1995, p. 276.

[36] D.W. Boo, W.S. Oh, M.S. Kim, K. Kim, H.-C. Lee, Chem. Phys. Lett. 120 (1985) 301.

[37] P. Matejka, J. Stavek, K. Volka, B. Schrader, Appl. Spectrosc. 50 (1996) 409.

[38] Y. Kurokawa, Y. Imai, Y. Tamai, Analyst 122 (1997) 941.

[39] M. Kim, K. Itoh, J. Electroanal. Chem. 188 (1985) 137.

[40] R.P. Cooney, M.R. Mahoney, M.W. Howard, Langmuir 1 (1985) 273.

[41] S. Oe, K. Fukushima, J. Mol. Struct. 223 (1990) 337.

[42] A. Hamelin, in: B.E. Conway, R.E. White, J. O'M Bockris (Eds.), Modern Aspects of Electrochemistry, vol. 16, Plenum Press, New York, 1985, p. 1.

[43] A. Hamelin, J. Electroanal. Chem. 407 (1996) 1.

[44] A. Moissette, Y. Batonneau, C. Bremard, J. Am. Chem. Soc. 123 (2001) 12325.

[45] J.A. Craighton, Spectroscopy of Surfaces—Advances in Spectroscopy, vol. 16 (Ch. 2), Wiley, New York, 1988, p. 37.

[46] P. Gao, M.J. Weaver, J. Phys. Chem. 89 (1985) 5040.

[47] A. Bogozi, O. Lam, H. He, C. Li, N.J. Tao, L.A. Nagahara, I. Amlani, R. Tsui, J. Am. Chem. Soc. 123 (2001) 4585.

[48] H.X. He, C. Shu, C.Z. Li, N.J. Tao, J. Electroanal. Chem. 522 (2002) 26.

[49] W.R. Fawcett, M. Fedurco, K. Kováčová, Z. Borkowska, Langmuir 10 (1994) 912.

[50] R.F. Dallinger, W.H. Woodruff, J. Am. Chem. Soc. 101 (1979) 4391.

[51] P.K. Mallick, G.D. Danzer, D.P. Strommen, J.R. Kincaid, J. Phys. Chem. 92 (1988) 5628.

[52] A.G. Brolo, D.E. Irish, G. Szymanski, J. Lipkowski, Langmuir 14 (1998) 517.

[53] S.A. Chaffins, J.Y. Gui, B.E. Kahn, C.H. Lin, F. Lu, G.N. Salaita, D.A. Stern, D.C. Zapien, A.T. Hubbard, Langmuir 6 (1990) 957.